ORIGINAL ARTICLE

Effect of double-excitation ultrasonic elliptical vibration turning trajectory on surface morphology

Bingjun Huo[1] · Bo Zhao[1] · Long Yin[1] · Xingchen Guo[1] · Xiaobo Wang[1]

Abstract

To explore the formation law and influence factors of three-dimensional geometry in axial turning surface, the turning experiment of 7075 aluminum alloy was carried out by using double excitation three-dimensional ultrasonic elliptical vibration method. Based on the theory of turning kinematics, the tool tip trajectory model of three-dimensional ultrasonic elliptical vibration turning (3D-UEVT) was established, and the related mechanism in surface residual height, surface topography formation characteristics, and turning transmission was given. Through single factor simulation and turning test, the influence of spindle speed, feed speed, amplitude, and phase difference on the surface microstructure and roughness of workpiece was analyzed contrastively. The results show that, compared with the traditional turning, the double excitation ellipse assisted turning can affect the surface topography and quality of the workpiece by causing the dynamic change of the cutting angle of the tool tip and the residual height of the material. Combined with the analysis of simulation and experimental results, it is found that the ideal microstructure and roughness can be obtained with low speed, slow feed, small amplitude, and small phase difference. Meanwhile, the tool workpiece separation characteristics, surface topography, roughness, and surface defect level can be effectively improved under the three-dimensional ultrasonic elliptical assisted vibration.

Keywords 7075 Aluminum alloy · Double-excitation ultrasonic elliptical vibration method · Surface roughness · Surface topography · Tool tip trajectory model

1 Introduction

Surface topography, also known as surface micro-geometry, refers to the surface roughness, waviness, shape error, texture, and other irregular micro-geometrical shapes [1, 2]. The special machined surface topography can improve the wear resistance, reliability, and service life of the mechanical part. Proper stipulation and control of the surface topography often have no less effect than the use of new materials and new structures [3, 4]. The requirement of surface topography with special surface texture characteristics is growing with the development of precision and ultra-precision manufacturing. Therefore, seeking new processing methods is necessary.

Ultrasonic elliptical vibration cutting is a new type of special surface texture processing method [5]. Ultrasonic elliptical vibration was attached to the tool to vibrate the tool tip in an elliptical trajectory relative to the workpiece, thereby realizing high-frequency intermittent vibration cutting. In the actual machining process, the ultrasonic elliptical vibration cutting trajectory is affected by the amplitude, tool shape, cutting speed, and phase difference, which, in turn, affects the actual machining quality [6]. The phenomenon of periodic separation of cutting workpieces has changed the existing traditional cutting methods, and also overcomes the problem that the cutting force can only be reduced by ultra-high-speed cutting and tool sharpening in traditional cutting [7, 8]. Meanwhile, ultrasonic elliptical vibration cutting (UEVC) also has the

✉ Bo Zhao
zhaob@hpu.edu.cn

Bingjun Huo
286452560@qq.com

Long Yin
916492657@qq.com

Xingchen Guo
15738515767@163.com

Xiaobo Wang
wangxb@hpu.edu.cn

[1] School of Mechanical and Power Engineering, Henan Polytechnic University, Jiaozuo 454000, Henan, China

characteristics of improving the shape accuracy of the parts with weak stiffness and the stability of the workpiece system, inhibiting burrs and delaying tool wear [9–11]. The three-dimensional (3D) ultrasonic elliptical vibration cutting can produce surface morphologies with complex micro-nano structures, making the workpiece have special mechanical, physical, chemical, and biological properties, such as reflectivity, adhesion, friction, and hydrophobicity [12–15].

Many scholars have explored the ultrasonic elliptical vibration cutting system. Luan et al. [16] used single excitation to study the surface quality and topography characteristics of unidirectional ultrasonic vibration turning of 7075-T6 aluminum alloy. They found that ultrasonic vibration cutting had an ironing effect on the processed surface, thereby reducing the residual area height and surface roughness of the machined surface. Later, Tong et al. [17] used a single-excitation super-elliptical vibratory turning system to study the surface topography of aluminum alloy. They established a tool motion trajectory model and found that the feed rate and amplitude had a significant impact on the surface topography. Huang et al. [18] established a machining model for elliptical vibration turning brittle materials and analyzed the influence and mechanism of ultrasonic elliptical vibration processing parameters on the micro-groove insert cutting process. However, the geometric mathematical model and finite element simulation analysis of elliptical vibration cutting are insufficient. Lu et al. [19] established a 3D micro-surface geometry model from a geometric point of view. They analyzed the influence of relevant cutting parameters on the surface topography of Ti6A14V alloy and found that the surface topography showed a deteriorating trend with the increase in the feed rate in the X and Y directions. Zhang et al. [20] proposed an ultrasonic elliptical vibration–assisted cutting technology based on a micro-texture model to produce mixed micro-textures with different geometric characteristics. The mathematical calculation of the cutting trajectory and the analysis of the mixed notch shape were performed to verify the correctness of the technology.

Regarding the influence of elliptical vibration cutting parameters on machining, Kong et al. [21] studied the performance of American Iron and Steel Institute 1045 steel in elliptical vibration cutting using a finite element simulation method to investigate the influence of elliptical vibration cutting parameters on machining. They studied the influence of frequency and amplitude on the cutting force, residual stress, and temperature. Cao et al. [22] studied the micro-texture simulation of aluminum alloy surface based on ultrasonic elliptical vibration–assisted turning, built a theoretical model reflecting the micro-texture surface, and carried out simulation experiments. They analyzed the influence of processing parameters and ultrasonic parameters on the micro-texture geometry size. Yuan et al. [23] studied the micro-texture and its characteristics on the surface of 7075 aluminum alloy by elliptical vibration–assisted turning. They analyzed the variation

law of micro-texture under different rotating speeds and feed speeds, and found that the geometric size and surface roughness of micro-texture changed regularly with the change in processing parameters. In terms of turning tools, Zhang et al. [24] studied the process of artificial polycrystalline diamond (PCD) tool turning hardened steel with ultrasonic elliptical vibration. They found that the cheap PCD tool could replace the single crystalline diamond tool for experimental processing under ultrasonic elliptical vibration cutting technology, effectively obtaining a good surface quality.

In the experiment of elliptical vibration cutting phase angle change, Zhu et al. [25] established a model of the influence of phase difference on cutting performance in ultrasonic elliptical vibration cutting. They found that the phase offset was sinusoidally related to the critical speed ratio and was not related to other ultrasonic parameters. Jiang et al. [26] established the model of the residual height along cutting direction caused by the change in the elliptical vibration cutting track, the model of the influence of dynamic cutting angle change on the machined surface quality. They found that the deflection change in the ultrasonic elliptical vibration cutting path was an important factor leading to the change in the cutting surface quality, but the phase difference change in the turning experiment was not fully analyzed.

In view of the aforementioned problems, this study analyzed the principle of double-excitation 3D ultrasonic elliptical vibration and the motion characteristics of the tool-tip trajectory under different cutting parameters. A 3D turning profile simulation model was established to verify the motion characteristics of trajectory. Based on 7075 aluminum alloy material, experiments were carried out by using the double-excitation 3D-ultrasonic elliptical vibration turning (3D-UEVT) system. Its results showed the influence and formation mechanism of the tool-tip trajectory on the machined surface quality of 7075 aluminum alloy under different rotational speeds, feed speeds, ultrasonic amplitudes, and phase difference parameters. Also, the obtained machined surface topography was analyzed.

2 3D-UEVT principle and topography simulation

2.1 Double-excitation UEVT motion analysis

Ultrasonic elliptical vibration cutting trajectory is composed of an ultrasonic tool vibration track and a spindle-driven workpiece rotation trajectory, as shown in Fig. 1. In this experiment, the 3D-UEVT was done in two vertical directions of X and Y to give the tool two vibration sources. Therefore, the vibrations in the two orthogonal directions were coupled to the position of the tool tip, forming a third direction resonance, thereby superimposing and synthesizing a 3D elliptical
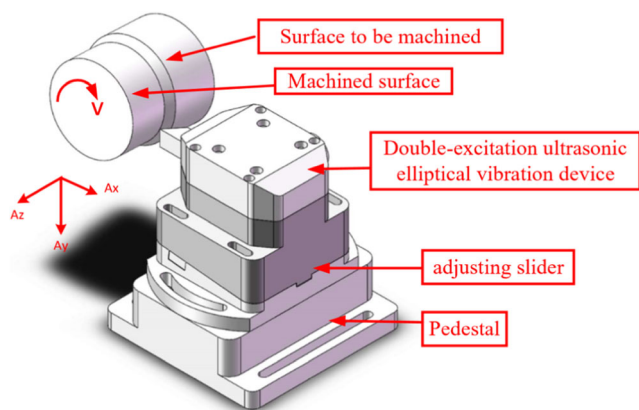
Fig. 1 Double-excitation 3D-UEVT model

vibration cutting trajectory. The motion trajectory equation is:

$$\begin{cases} X = A_x\sin(2\pi ft + \phi_x) \\ Y = A_y\sin(2\pi ft + \phi_y) \\ Z = A_z\cos(2\pi ft + \phi_z) \end{cases} \quad (1)$$

where A_x, A_y, and A_z are amplitudes in X, Y, and Z directions. φ_x, φ_y, and φ_z are angular phase shifts in X, Y, and Z directions. f is the vibrational frequency of the tool, and t is the cutting time. The 3D-UEVT motion track is shown in Fig. 2 under the raw state. The shape and deflection of the elliptical vibration cutting path could be changed by controlling the amplitude and phase difference. By controlling only the phase difference, the elliptical vibration cutting path of the tool tip could be obtained, as shown in Fig. 3.

In the actual machining process, the vibration of the tool in the depth of cut and the theoretical cutting depth determines the actual cutting depth of the tool. The vibration and cutting speed of the tool in the cutting direction determine the actual cutting speed of the tool on the workpiece. The vibration in the feed direction and the theoretical feed rate determine the relative feed rate. Therefore, the 3D elliptical vibration trajectory
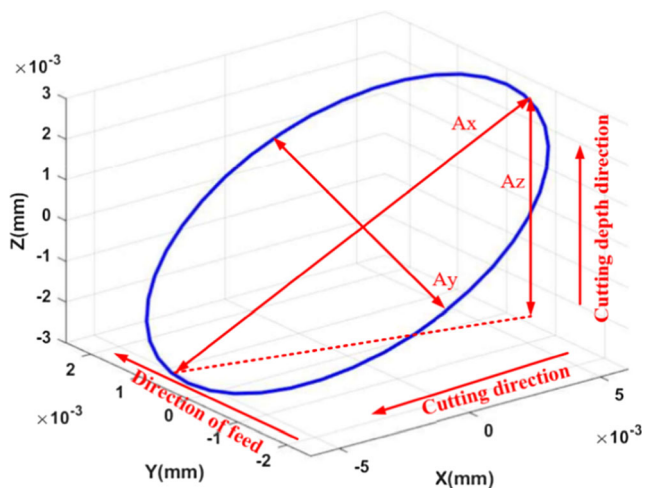

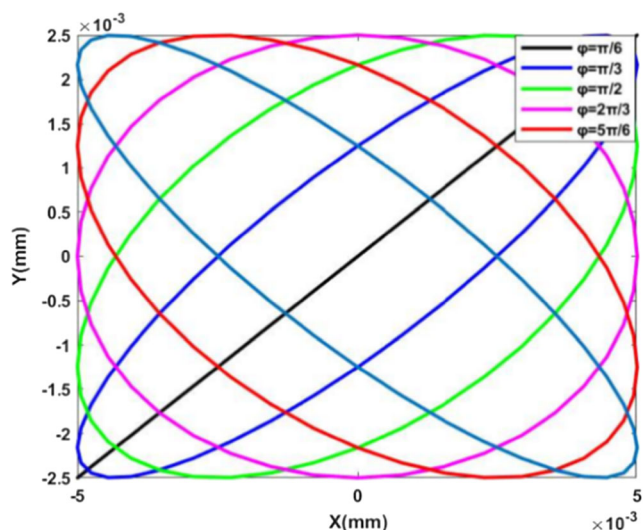Fig. 2 Elliptic vibration cutting trajectory in the unprocessed state

Fig. 3 Elliptic vibration cutting paths with different phase differences

of the tool due to the vibration in these three directions made the turning surface produce a unique "fish scale" surface topography. The cutting process is shown in Fig. 4. Therefore, the trajectory equation of the double-excitation 3D-UEVT tool could be expressed as:

$$\begin{cases} X' = A_x\sin(2\pi ft + \phi_x) - a_p \\ Y' = A_y\sin(2\pi ft + \phi_y) + V_c \cdot t \\ Z' = A_z\cos(2\pi ft + \phi_z) + V_f \cdot t \end{cases} \quad (2)$$

where a_p represents the depth of the cut, V_c represents the linear cutting speed, and V_f represents the tool feed speed.

According to Eq. (2), the cutting speed components of tool is expressed as:

$$\begin{cases} V_x(t) = 2\pi f A_x\cos(2\pi ft + \phi_x) \\ V_y(t) = 2\pi f A_y\cos(2\pi ft + \phi_y) + V_c \\ V_z(t) = -2\pi f A_z\sin(2\pi ft + \phi_z) + V_f \end{cases} \quad (3)$$

The instantaneous cutting speed $V_t(t)$ of the tool is:

$$V_t(t) = \sqrt{V_x(t)^2 + V_y(t)^2 + V_z(t)^2} \quad (4)$$

Equations (3) and (4) show that the cutting speed of the tool movement could be determined by the combination of the machine tool's own cutting speed V_c and feed rate V_f and the ultrasonic elliptical vibration Eq. (1). The tool had a critical instantaneous cutting speed V_{MAX}. When the actual cutting speed V_t was greater than the critical instantaneous cutting speed V_{MAX}, the tool was not able to effectively separate and cut the workpiece.

As shown in Fig. 5, a simulation of the turning motion trajectory of the tool tip in the machine tool coordinate system was established by Eq. (2). The actual cutting depth of the UEVT tool tip in the X direction was determined using the amplitude and the deflection angle of the phase difference due

Fig. 4 Schematic diagram of
ultrasonic elliptical vibration
cutting
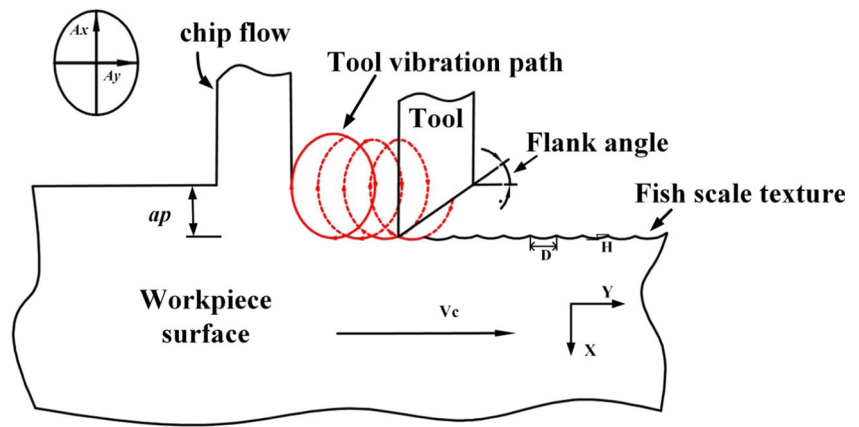
to the dynamic change of the tool-entry angle, altering the influence of the ultrasonic turning tool path and residual height. When the actual cutting speed of the tool tip in the Y direction was greater than the theoretical cutting speed, the tool–workpiece cycle separation characteristics disappeared. The actual feed speed of the tool tip in the Z direction exhibited a partial periodic retreat, thereby showing an ironing effect on the processed surface.

2.2 3D-UEVT tool tip trajectory analysis

Compared with the one-dimensional and two-dimensional ultrasonic turning cutting edge trajectories, the change in 3D ultrasonic elliptical vibration cutting edge trajectory was more complex, and the change in different parameters affected its motion characteristics and cutting characteristics. Therefore, according to Eq. (2), the 3D ultrasonic elliptical vibration tooltip motion equation, the change law of the tool-tip trajectory was simulated using matrix laboratory (MATLAB).
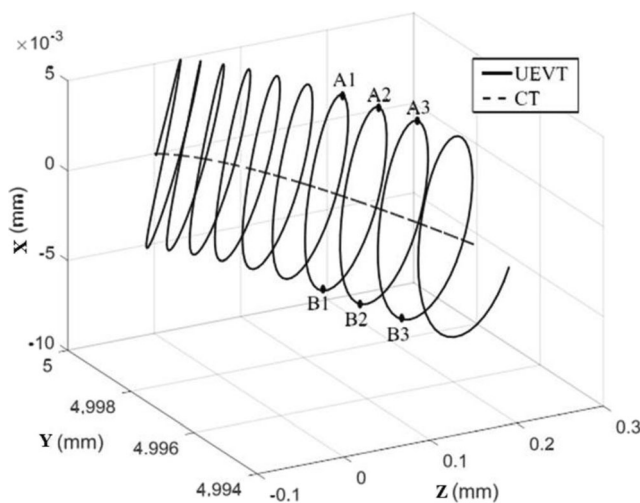
As double-excitation UEVT tool tip motion trajectory is complicate, it fails to accurately model the space topographic by Boolean operations. Therefore, the workpiece meshing method and "reduction approximation algorithm" [27] are attempted to solve the issue.

Figures 6 and 7 show the influence of machining parameters with different rotational speeds and different feed speeds, respectively, on the trajectory of cutting edges in unit time. Figure 6 shows that when the spindle speed was low, the turning phenomenon of cutting edge motion track was more obvious. The rotation of the cutting edge gradually weakened, the length of the path from the tool–workpiece separation to the combination gradually reduced, and the net cutting time during the ultrasonic vibration cycle gradually increased with the increase in the spindle speed. When the cutting speed exceeded the critical cutting speed V_{MAX}, the motion path of the cutting edge no longer appeared to rotate, and the tool–workpiece no longer had the characteristic of separation. Figure 7 shows that when only the feed rate is increased, the span of the tool nose trajectory in the feed direction (Z direction) increases. When the feed speed was low, the workpiece
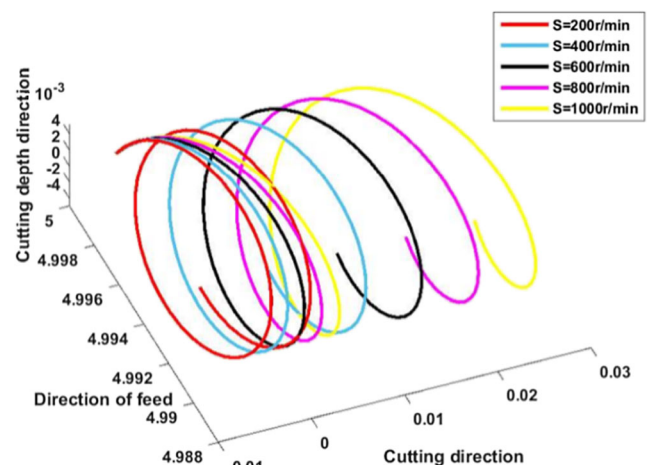

Fig. 5 Spatial motion trajectory simulation of knife tip

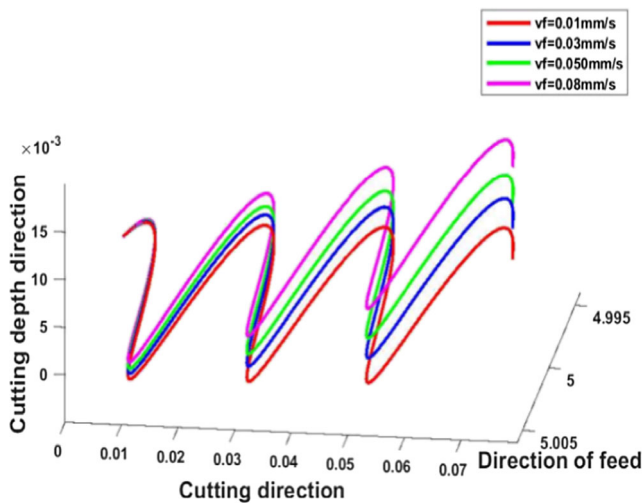**Fig. 6** Tool tip trajectory at different speeds

Fig. 7 Tool nose motion path at different feed speeds

underwent high-frequency elliptical turning in the circumferential unit area many times. When the feed speed increased, the turning times in the circumferential unit area decreased, and the feed speed had no change in other directions. This finding confirmed that the change in the feed rate only affected the cutting edge path in the feed direction.

Figures 8 and 9 show the influence of acoustic parameters, such as different vibration amplitudes and phase differences, on tool tip trajectory in unit time, respectively. Figure 8 shows that as the amplitude increased, the tool–workpiece separation phenomenon became more obvious. As the amplitude of the tool changed in all directions, ultrasonic elliptical vibration cutting showed periodic changes from elliptical cutting to round cutting, and the range of actual cutting depth increased as the amplitude of the cutting tool increased in all directions. Figure 9 shows that when the phase difference changed, the trajectory of the cutting edge changed greatly. Moreover, different phase differences also affected the dynamic change in the cutting angle of the tool, combined with the "ironing" effect of the edge of the tool, thereby affecting the residual
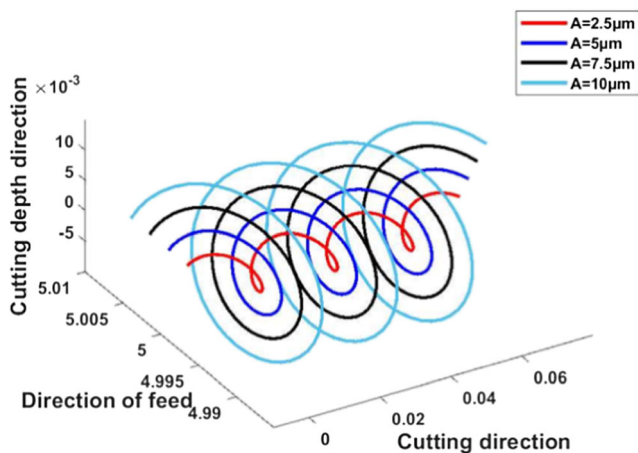

Fig. 8 Tool tip motion trajectory at different amplitudes

height and surface roughness. Under the phase difference change, the tool vibration trajectory and the cutting angle changed the actual cutting depth, as shown in Fig. 10.

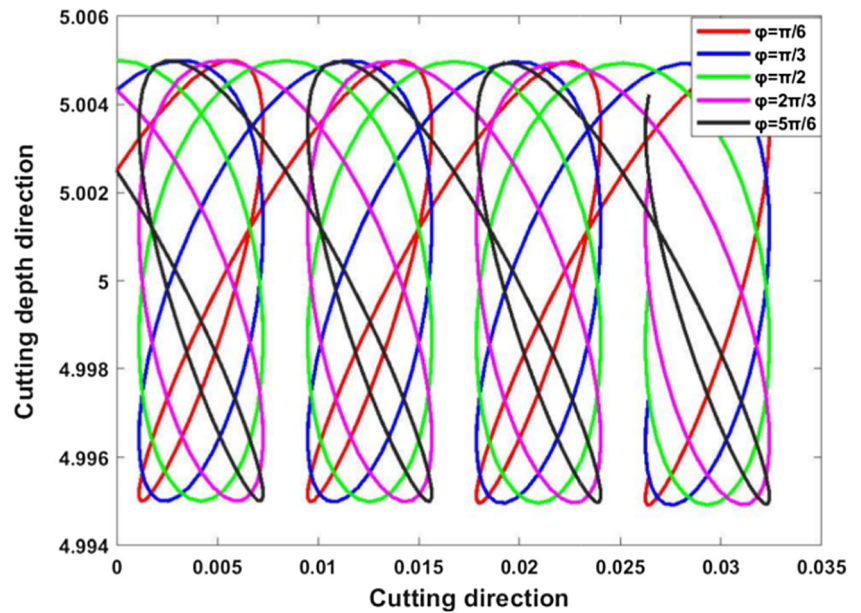## 2.3 3D shape simulation of double-excitation UEVT

The formation process of turning surface topography is the process in which the cutting edge reproduces the tool contour to the machined surface along a certain motion path. Its essence is the process in which the cutting edge moves on the machined surface and forms the surface topography. It follows the principle of edge shape remapping and the cutting interference effect of cutting tools. The tool and its enveloping surface move in the volume of the workpiece, and any intersection volume between the tool and the workpiece is subtracted from the volume of the workpiece, leaving the path of the cutting edge in the workpiece. The MATLAB software is used to simulate the microstructure of a 3D-UEVT surface, and different vibration modes and processing parameters are simulated and verified.

Through MATLAB simulation, some 3D surface maps were extracted; the simulation results under different parameters are shown in Fig. 11.

As shown in Fig. 11a–c, the spindle speed parameter gradually increased from $n = 200$ to $n = 600$ r/min. The analysis shows that the distance between the surface micro-texture remnants gradually increases in the cutting direction, and the width of the joint of the residual height of the micro-textured unit also increased obviously. As shown in Fig. 11b, d, and e, the feed speed gradually increased from $V_f =10$ to $V_f = 30$ μm/r. The analysis shows that the residual height of machined surface topography gradually increased, and the cutting times per unit area decreased accordingly. As shown in Fig. 11b, f, and g, the amplitudes were $A_x = 2$ μm, $A_x = 3$ μm, and $A_x = 4$ μm, respectively. The analysis shows that the surface micro-texture size became larger, and the actual cutting depth gradually increased. As shown in Fig. 11b, h, and i, the phase angles were 60°, 30°, and 90°, respectively. The analysis shows that the micro-texture shape in the cutting direction and the feeding direction and the angle of the central axis of the elliptical groove changed with the change in the phase angle, which affected the actual cutting depth.

According to the results of MATLAB simulation, when selecting different processing parameters, the surface micro-texture in the feeding direction and the cutting direction and the cutting depth was affected to a certain extent. When the parameter changes had a great influence on the trajectory, the tool–workpiece separation characteristic appeared in the trajectory, leading to a self-intersecting superimposed removal phenomenon. The formation mechanism and change the law of the surface topography of 3D-UEVT processing could be effectively predicted by changing different processing

Fig. 9 Tool tip motion trajectory at different phase differences

parameters and acoustic characterization parameters for simulation calculation.

3 Experimental verification of double-excitation UEVT

3.1 Experimental equipment and conditions

The experiment was performed using a self-developed single double-excitation ultrasonic generator to realize ultrasonic vibration with double-excitation sources at the same frequency to verify the accuracy of the tool-tip trajectory and surface topography simulation in Section 2. The experimental device of UEVT is shown in Fig. 12. The machine tool used in the

Fig. 10 Elliptic vibration cutting trajectory deflection

experiment was SPHERE 360, the cutting method was cylindrical cutting, and the ultrasonic vibration directions were feeding direction vibration, cutting direction vibration, and cutting depth vibration. The experimental conditions are shown in Table 1. The turning test was used to study the surface topography and surface characteristics of 3D-UEVT, and the single-factor test was used to study the influence of vibration and processing parameters of 3D-UEVT on the machined surface topography. The experimental parameters are shown in Table 2.

This article selects the laser displacement sensor model KEYENCE LK-G10 to measure the amplitude of the UEVT device. The system mainly includes a LK-G10 series laser main controller, laser displacement sensor, the LK-Navigator operating software, and computer terminal. When testing the amplitude and the tool tip vibration trajectory, focus the laser beam on the tool tip X, Y, and Z planes respectively. After the ultrasonic vibration system is started for 15 min and stabilized, the vibration measurement is carried out: once every 5 min, the measurement is conducted three times. The measurement site is shown in Fig. 13.

The processing material is 7075 aluminum alloy for aviation, and the material performance parameters are shown in Table 3.

After the processed workpiece is cleaned by an ultrasonic cleaning machine, the quality of the processed surface is measured with optical inspection equipment. The micro-morphology of the machined surface was observed by KEYENCE kearns VHX-500FE ultra-depth microscope, and the roughness value Ra of the machined surface was measured and the surface profile data was collected by Taylorsurf CCI6000 noncontact 3D white light interference surface profiler. The optical inspection equipment is shown in Fig. 14.
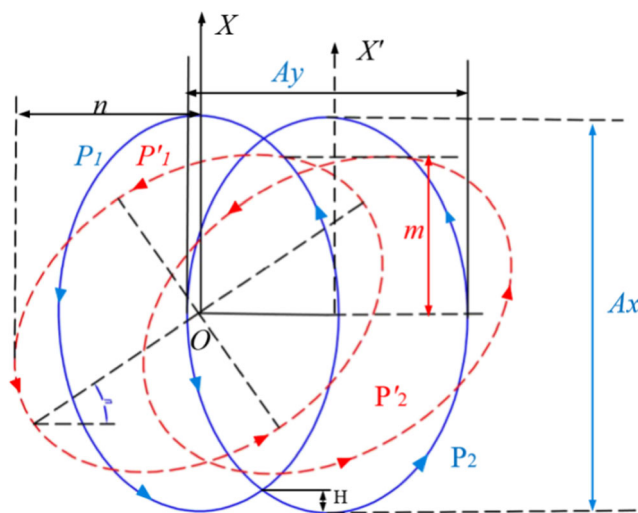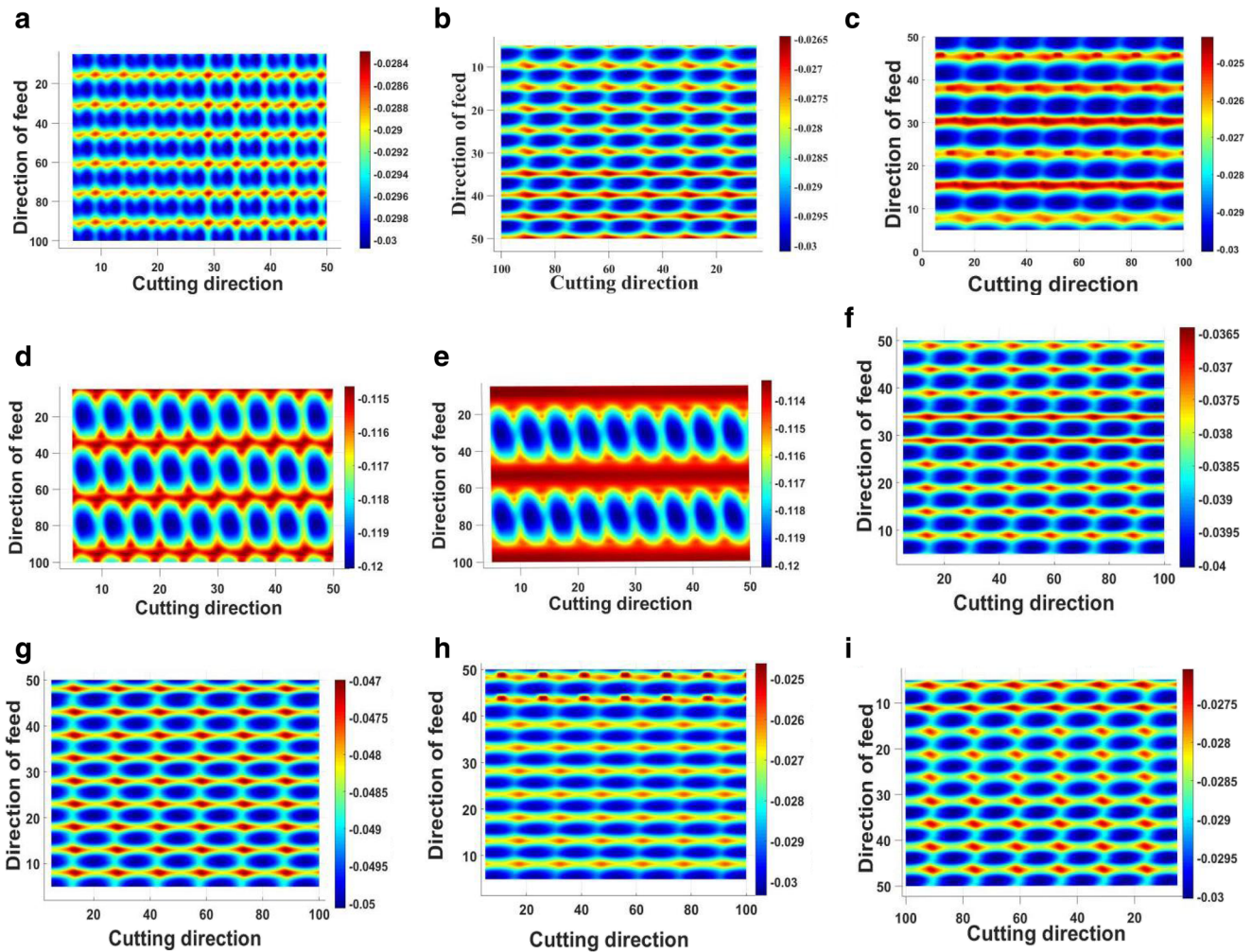
Fig. 11 Simulation diagram of surface topography with different parameters. a n=200 r/min, **b** n=400 r/min, **c** n=600 r/min, **d** V_f=20 μm/r, **e** V_f=30 μm/r, **f** A_x=3 μm, **g** A_x=4 μm, **h** φ=30°, **i** φ=90°. The common parameters are the following: **a**, **b**, **c** a_p=10 μm, V_f=10 μm/r, A_x=2 μm, φ=60°; **b**, **d**, **e** n=400 r/min, a_p=10 μm, A_x=2 μm, φ=60°; **b**, **f**, **g** n=400 r/min, a_p=10 μm, V_f=10 μm/r, φ=60°; **b**, **h**, **i** n=400 r/min, a_p=10 μm, V_f=10 μm/r, A_x=2 μm)

3.2 Experimental verification and comparison

Under the above experimental conditions, observe and analyze the processed surface. Under the same parameters, the
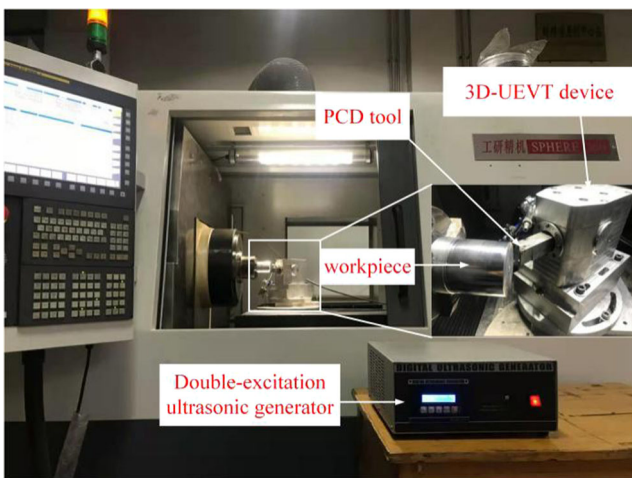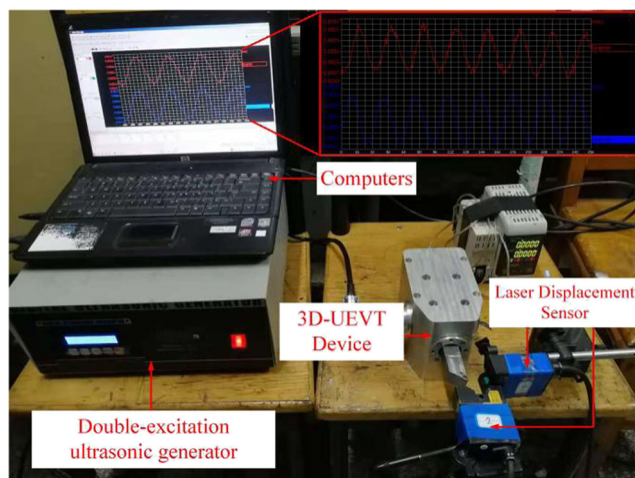

Fig. 12 3D ultrasonic elliptical vibration-assisted turning experiment platform

Table 1 Experimental conditions

Designation	Parameters
PCD tool	Hook angle 0°
	Relief angle 11°
	Tool cutting edge angle 62. 5°
	Corner radius 1.0 mm
f/KHz	24.95
Workpiece material	7075 Aluminum alloy
Cutting fluid	Kerosene oil mist

Table 2   The parameters of the 3D-UEVT experiment

Serial number	$n/(\text{r}\cdot\text{min}^{-1})$	$V_f/(\mu\text{m}\cdot\text{r}^{-1})$	$a_p/(\mu\text{m})$	$A_x/(\mu\text{m})$	$\varphi/(°)$
1	200	10	10	2.0	90
	400				
	600				
	800				
2	800	10	10	2.0	90
		20			
		30			
		40			
3	800	10	10	2.0	90
4	800	10	10	1.5	90
				2.0	
				2.5	
				3.0	
5	800	10	10	2.0	30
					60
					90
					120

Table 3   Properties of 7075AL

Density $\rho(\text{kg/m}^3)$	Extension	Hardness (HB)	Yield strength (MPa)	Tensile strength (MPa)	Thermal coefficient of expansion
2800	11	15	503	527	23.6E-006

texture, and it is evenly distributed on the current measurement surface. As shown in Fig. 15c and d.

Figure 16 presents the micro-topography of the machined surface with different spindle speeds, n=200, 400, 600, and 800 r/min, measured using a digital microscope (KEYENCE, Japan, VHX-500FE). Compared with the second section 2.3, the ultrasonic vibration turning presents a interferes between three-dimensional elliptical harmonic motion and the tool tip, by only changing spindle speed. That resulted in the regular mesh shape on the machined surface, as well as the sharp wave peaks at the intersection of the grids. However, as the cutting speed exceeded the critical cutting speed, the actual cutting time increased gradually within an ultrasonic vibration cycle. The tool, therefore, failed to separate against the workpiece. It led to the ironing effect of the tool primary flank face on the machined face, thereby reducing the residual height, and that was supported by the simulation results. It is verified that the model could more accurately indicate the changing trend of surface topography in the actual cutting.

When the spindle speed n=400 r/min, the cutting depth a_p=10 μm, the feed speed V_f=10 μm/r, the X-direction amplitude A_x=2.0 μm, and the phase difference φ=60°, the 3D simulation surface of the machined surface and the machined surface are shown in Fig. 17. The microstructure of the machined surface is basically consistent.

KEYENCE kearns VHX-500FE ultra-depth microscope is used to observe the surface of traditional machining and 3D-UEVT workpieces at ×1000 magnification. It can be found that the micro-surface textures formed by the two machining methods are quite different. The cutting marks on the surface after traditional processing appear as parallel lines, while the cutting marks on the surface after 3D-UEVT processing appear as periodically distributed fish-scale lines, as shown in Fig. 15 a and b. In order to further compare and observe these two processing methods, a Taylorsurf CCI6000 noncontact 3D white light interference surface profiler was used to observe the 3D surface topography. Compared with traditional machining, the surface after three-dimensional ultrasonic elliptical vibration turning has an "elliptical groove"-like micro-

4 The influence of tool tip trajectory on surface topography

The aforementioned model showed that both processing and ultrasonic parameters affected the formation of surface topography. The influence mechanism of the tool-tip trajectory on surface topography has been analyzed in this section.

The arithmetic mean deviation Ra parameter was used to characterize and measure the surface roughness. The Taylorsurf CCI6000 noncontact 3D white light interference profilometer was used to measure the surface roughness of the workpiece. Under each parameter condition, three measuring areas were taken, and the average value of Ra in the three sampling areas was taken as the reference data value. Figure 18 shows the influence of each parameter on the surface roughness Ra under the condition of single factor.
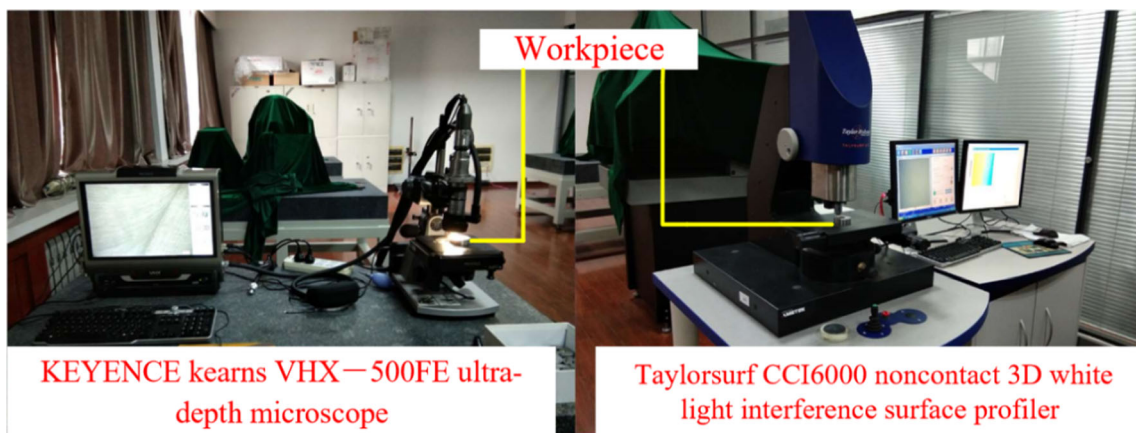

Fig. 13   Ultrasonic elliptical vibration measurement site diagram

Fig. 14 Optical inspection equipment

4.1 The influence of processing parameters on the microscopic morphology

In Fig. 18, the measurement results show that the surface roughness of the workpiece increased first and then decreased with the increase in the spindle speed when the other parameters remained unchanged. The workpiece surface roughness increased from 316.712 to 400.214 nm and then decreased to 308.531 nm, with a maximum change rate of 29.7%. The analysis shows that when the cutting speed increased gradually, the cutting length per unit time of the tool-tip path in the cutting direction increased, and the distance between the two adjacent micro-texture elements also increased. The rotary phenomenon of the cutting edge gradually weakened, and the tool and workpiece showed periodic contact and separation effect. However, when the cutting speed was higher than the critical cutting speed, the net cutting time in the ultrasonic vibration cycle increased gradually. The residual height of the machined surface decreased and the surface

roughness value decreased accordingly because of the "ironing" effect on the edge of the tool flank. In Fig. 18, the measurement results show that the roughness increased with the increase in the feed speed. The roughness increased from 270.651 to 486.042 nm, with an increase of 79.6%. Some experimental results are shown in Fig. 19. The analysis shows that when the feed speed was different, the tool nose trajectory presented different feed rates in the feed direction, which was reflected in the cutting state of the surface topography, which was the number of times of different elliptical turnings per unit area of the machined surface. When the feed speed was low, the unit area underwent multiple elliptical turnings, and the surface micro-texture self-intersection phenomenon occurred, which effectively reduced the residual height of the surface and the processed surface roughness value. When the feed speed increased, the number of turning times per unit area in the feed direction reduced, reducing the self-intersection of the micro-texture, and thus, the surface roughness value increased.
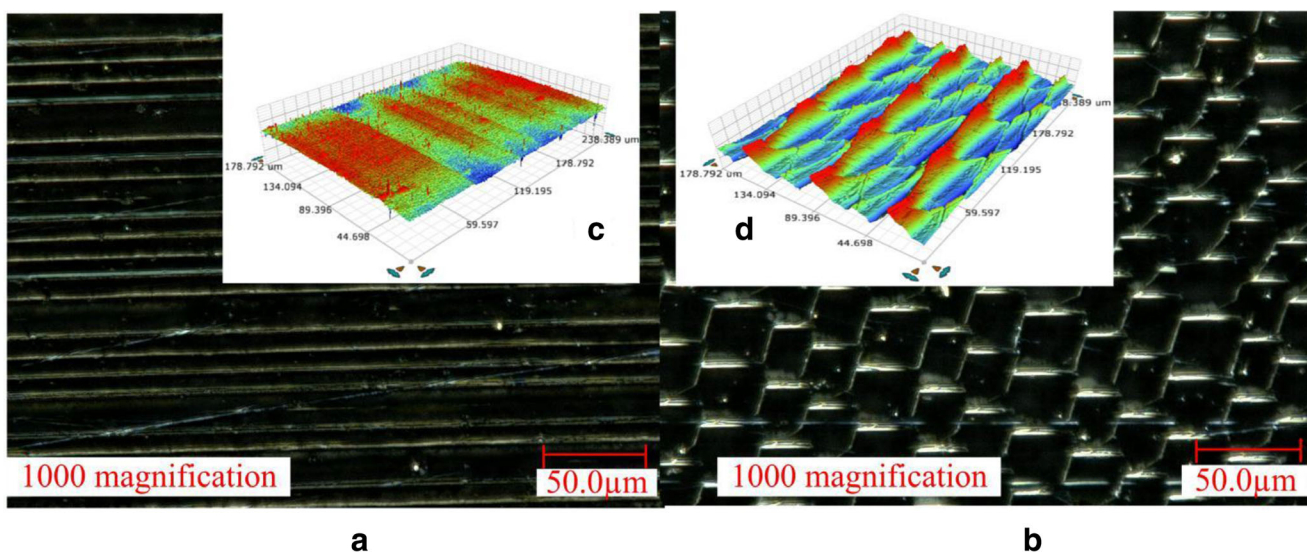

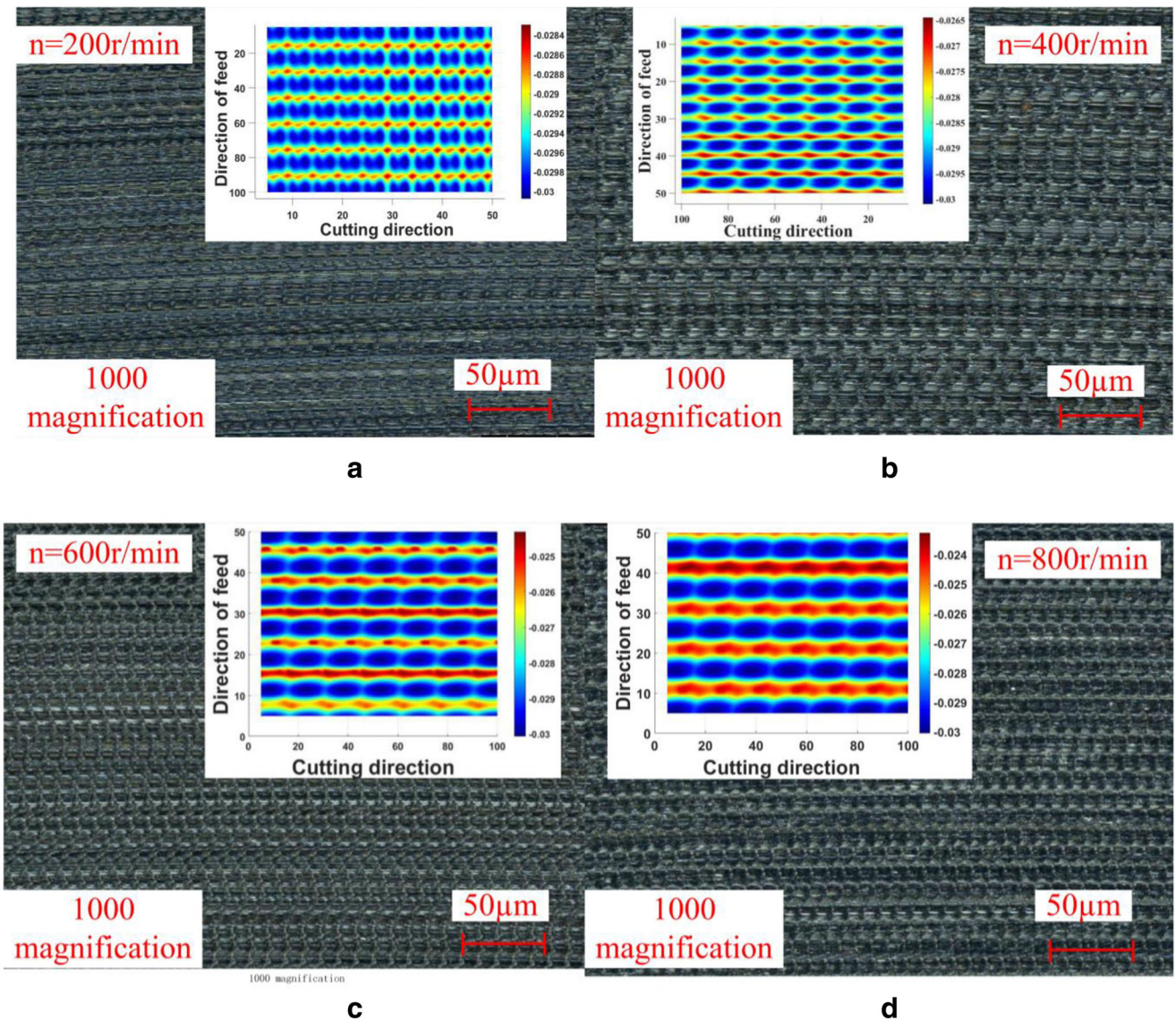**Fig. 15** Surface topography of CT and UEVT. **a** CT of micro-surface, **b** UEVT of micro-surface

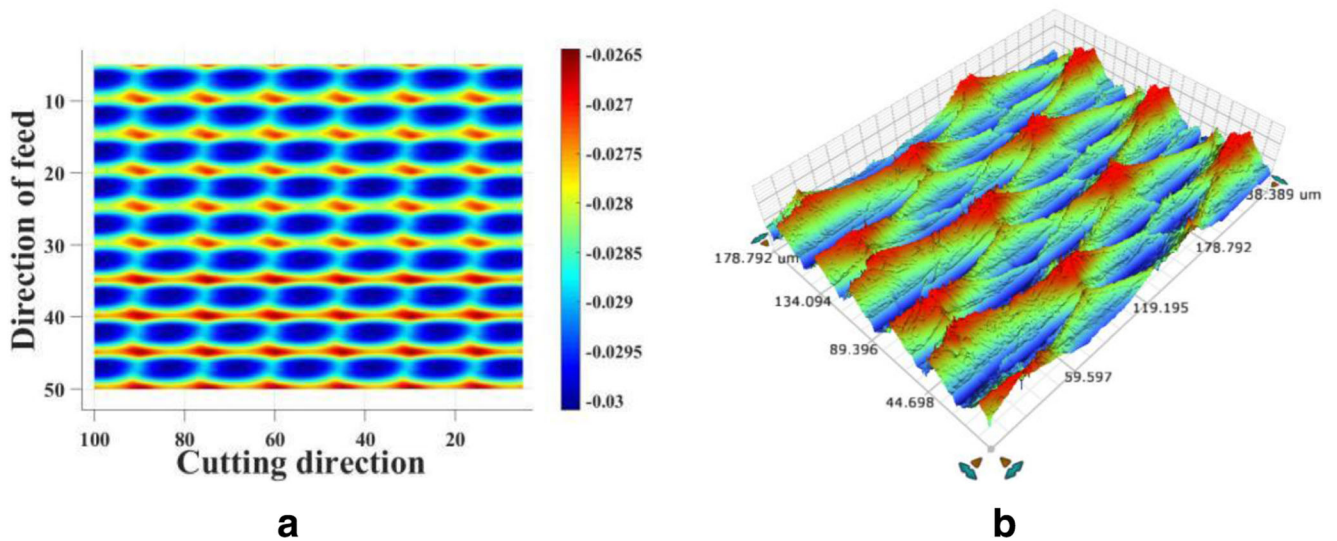**Fig. 16** Comparison of surface topography simulation results and experimental results

Fig. 17 Machining surface microstructure of 3D-UEVT. **a** Surface topography of simulate. **b** Surface topography of turning

Fig. 18 Influence of parameters on arithmetic mean deviation Ra of surface contour
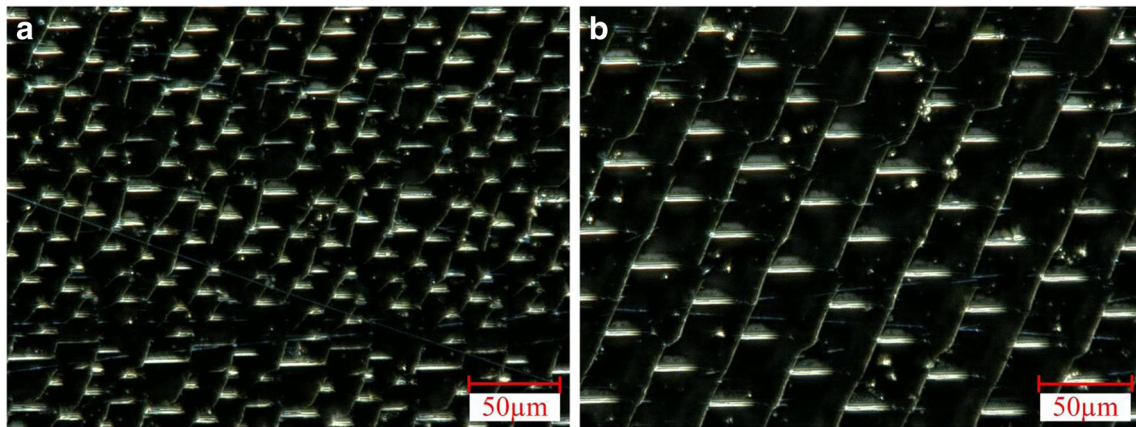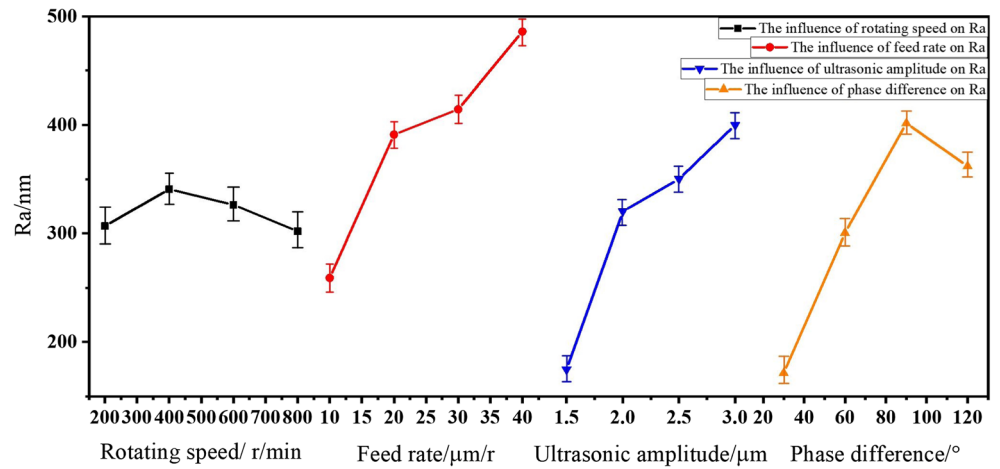

Fig. 19 Machining surface with different feed speeds. **a** V_f=5 μm/r, **b** V_f=20 μm/r (same parameters are the following: n=800 r/min, a_p=10 μm, V_f=10 μm/r, A_x=2 μm, φ=90°)

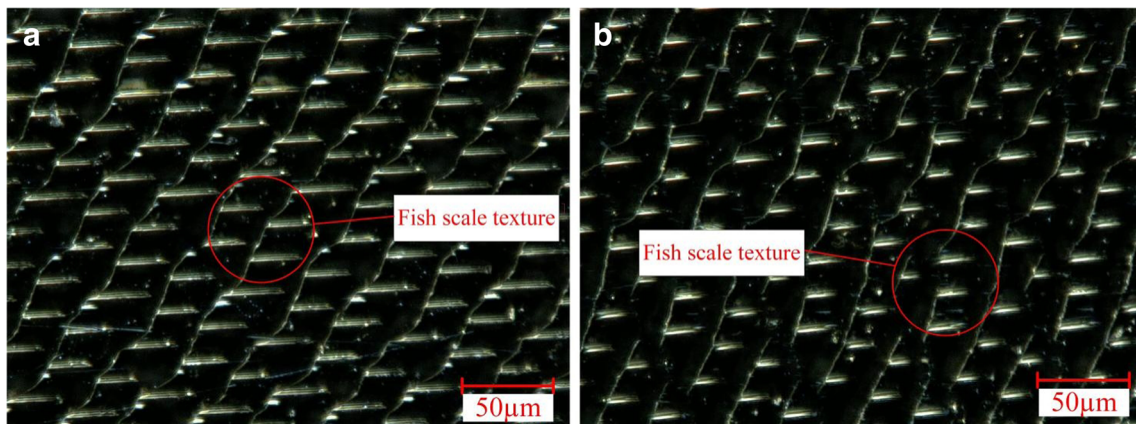**Fig. 20** Machining surface with different amplitudes. **a** A_x=1.5 μm, **b** A_x=3 μm (same parameters are the following: n=800 r/min, a_p=10 μm, V_f=10 μm/r, φ=90°)

4.2 The influence of ultrasonic parameters on the microscopic morphology

In Fig. 18, the measurement results show that the surface roughness of the workpiece also increased with the increase in the ultrasonic amplitude. The surface roughness of workpiece increases from 174.583 to 376.956 nm, with an increase of 115.9%. Some experimental results are shown in Fig. 20. The analysis shows that when the ultrasonic amplitude increased gradually, the tool-tip trajectory showed that the turning area of forming a 3D ellipse increased, and the cutting width in the feeding direction increased accordingly. As the ultrasonic amplitude changed, the actual cutting depth also changed, thus affecting the formation of machined surface topography. When the other parameters remained unchanged, the tool vibration trajectory and direction changed the actual cutting depth with the change in the phase angle. Therefore, the workpiece surface roughness increased first and then decreased. The analysis shows that when the phase difference changed, the motion trajectory of the cutting edge showed that the cutting edge of the tool presented different cutting states, and the cutting angle changed dynamically. In the cutting
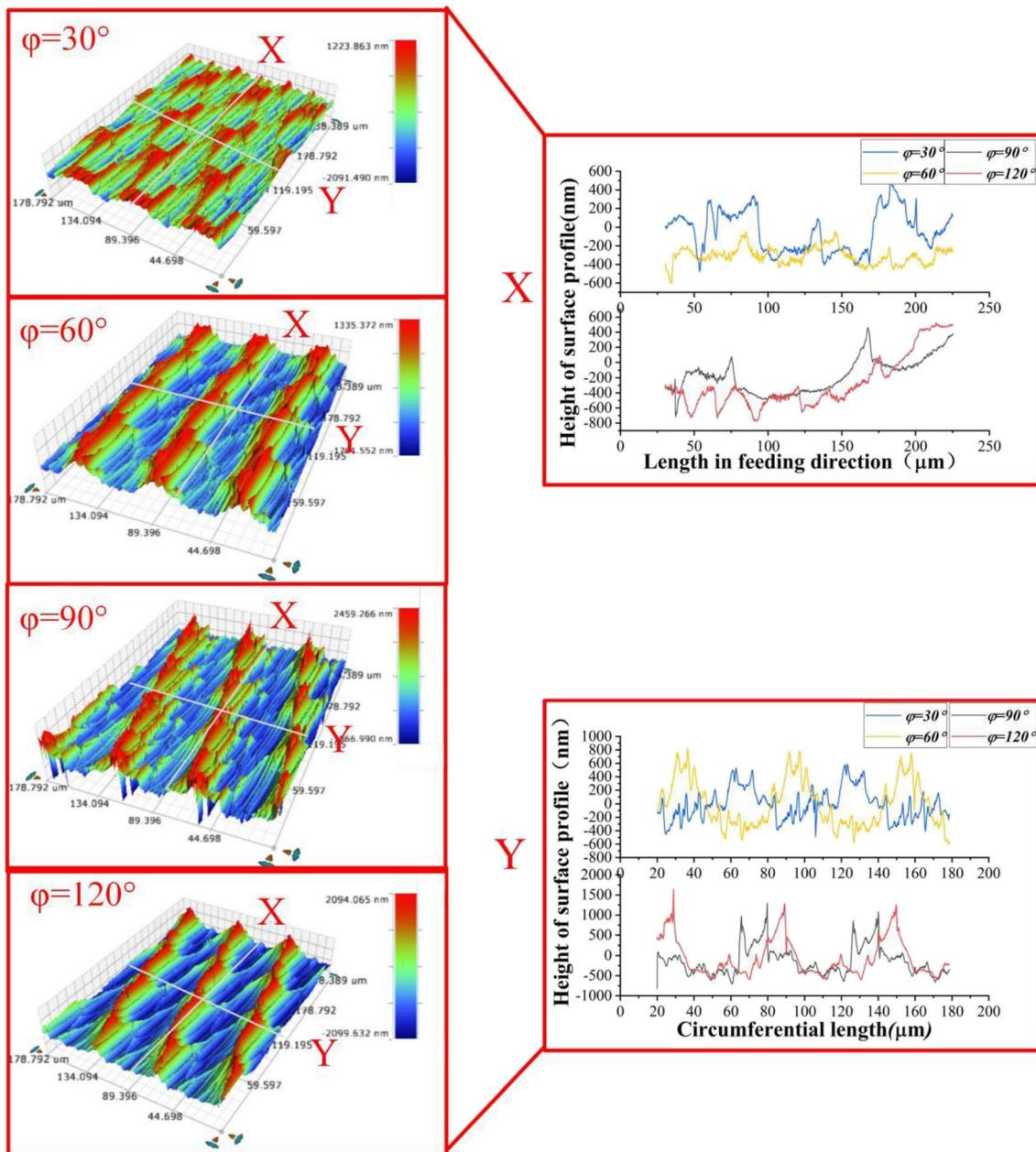

Fig. 21 Surface topography and profile curve with different phase differences. The rest of the parameters are the following: n=800 r/min, a_p=10 μm, A_x=2.0 μm, V_f = 10 μm/r

process, a certain self-intersection existed to repeat the cutting process, and the actual cutting depth of the tool also changed with the change in the phase difference, as shown in Fig. 10.

According to the above analysis, the surface profile quality in the cutting direction was affected by the cutting speed and phase difference. The surface profile quality in the feed direction was affected by the feed speed and ultrasonic amplitude. The analysis showed that better ultrasonic topography and roughness could be obtained with low spindle speed, low feed speed, low amplitude, and low phase angle, and the correctness of the analysis of surface topography formation mechanism was verified.

4.3 Analysis of surface roughness profile curves under different phase differences

In order to better analyze the influence of parameters on the surface roughness curve, the surface roughness profile curves with different phase differences are extracted and analyzed. Figure 21 shows the 3D surface topography and profile curve observed using a Taylorsurf CCI6000 noncontact 3D white light interference surface profiler with phase differences of $\varphi=30°$, $\varphi=60°$, $\varphi=90°$, and $\varphi=120°$. The measurement results show that when other parameters are unchanged, with the change of ultrasonic phase difference, in the circumferential direction of the workpiece, the difference of periodic fluctuation of the contour curve is small. With the increase of phase difference, the periodic fluctuation interval of profile curve has not changed greatly. When the phase angles are respectively $\varphi=30°$, $60°$, $90°$, and $120°$, the periodic intervals of the contour fluctuations are measured. The periodic fluctuation intervals between the contour curves are 67 μm, 60 μm, 64 μm, and 61 μm on average. However, the maximum peak value of the contour per unit length shows a regular change that first increases and then decreases. The maximum peak values of the contour curve per unit length are 555 nm, 754 nm, 1002 nm, and 1164 nm respectively. In the workpiece feed direction, with the increase of the phase angle, the periodic fluctuation interval of the contour curve changes obviously and regularly, and the contour height shows a law of first decreasing and then increasing. The maximum peak values of the contour per unit length are 490 nm, 490 nm, 672 nm, and 691 nm. It shows that during the 3D-UEVT processing, the change of the phase difference will cause the surface profile fluctuation curve and the maximum profile peak value to change.

5 Conclusions

The simulation model of the tool-tip trajectory and the prediction of surface topography in UEVT were established, and the formation mechanism of machined surface topography was studied and analyzed based on the trajectory kinematics model of ultrasonic elliptical vibration. The experiment of turning 7075 aluminum alloy was carried out using a double-excitation UEVT system, and the influence of the tool-tip trajectory on surface roughness under machining parameters and ultrasonic parameters was studied. The following conclusions were drawn:

(1) The trajectory of tool tip was analyzed in terms of machining parameters and ultrasonic parameters, and then, the prediction model of the machined surface topography was established. The tool tip and workpiece were discretized, by "reduction approximation algorithm," and the regular three-dimensional elliptical vibration micromorphology could be obtained. The analysis of the experimental results shows that the micro-morphology of the machined surface has the same change trend with the simulation results. The turning experiment verifies the correctness of the micro-morphology model of the double excitation ultrasonic elliptical vibration turning surface.

(2) The simulation results of double-excitation UEVT shown that the change in the tool-tip trajectory in double-excitation UEVT resulted in the change of the residual height along the cutting direction, as well as the actual cutting time, and the cutting depth.

(3) The mechanism of the spindle speed on the surface topography was the tool–workpiece separation characteristic in the cutting direction. In the feed direction, the mechanism of the feed speed on the surface topography was the self-intersection of the micro-texture per unit area. Ultrasonic amplitude changing the actual cutting depth was proportional to the surface roughness of the workpiece.

(4) In double-excitation UEVT, the tool vibration trajectory and direction changed the actual cutting depth with the change in phase difference, causing the surface roughness to increase first and then decrease. When the phase difference $\varphi = 30°$, an inhibitory effect on the residual height and burrs of the surface topography was observed, which had a positive effect on the surface microtopography.

Data availability The datasets used or analyzed during the current study are available from the corresponding author on reasonable request.

Declarations

Ethics approval and consent to participate The authors state that this paper is an original work, it has not been published in any journals, and this research does not involve any ethical issues of humans or animals. The authors declare that this research involves no Human Participants and/or Animals.

Consent for publication The authors confirm the paper described has not been published before; that it is not under consideration for publication elsewhere; that its publication has been approved by all co-authors; that its publication has been approved by the responsible authorities at the institution where the work is carried out. The authors agree to publication in the Journal indicated below and also to publication of the article in English by Springer in springer's corresponding English-language journal. The copyright to the English-language article is transferred to Springer effective if and when the article is accepted for publication. The author warrants that his/her contribution is original and that he/she has full power to make this grant. The author signs for and accepts responsibility for releasing this material on behalf of any and all co-authors. The copyright transfer covers the exclusive right to reproduce and distribute the article, including reprints, translations, photographic reproductions, microform, electronic form (offline, online), or any other reproductions of similar nature.

Competing interests The authors declare no competing interests.

References

1. Ulutan D, Ozel T (2011) Machining induced surface integrity intitanium and nickel alloys: a review. Int J Mach Tools Manuf 51(3):250–280
2. Dimogerontakis T, Vangils S, Ottevaere H, Thienpont HTH (2006) Quantitative topography characterization of surfaces with asymmetric roughness induced by AC-graining on Aluminium. Surf Coat Technol 201(3-4):918–926
3. Guo YB, Li W, Jawahir IS (2009) Surface integrity characterization and prediction in machining of hardened and difficult-to-machine alloys: a state-of-art research review and analysis. Mach Sci Technol 13:437–470
4. Cheharon CH, Jawaid A (2005) The effect of machining on surface integrity of titanium alloy Ti–6% Al–4% V. J Mater Process Technol 166:188–192
5. Ying N, Feng J, Bo Z, Guofu G, Jingjing N (2020) Theoretical investigation of machining-induced residual stresses in longitudinal torsional ultrasonicassisted milling. Int J Adv Manuf Technol 108(11-12):3689–3705
6. Jianguo Z, Tao C, Cheng G, Yongxin S, Huaijiang Y (2016) Review of micro/nano machining by utilizing elliptical vibration cutting. Int J Mach Tools Manuf 106:109–126
7. Kurniawan R, Kiswanto G, Jo Ko T (2017) Surface roughness of two-frequency elliptical vibration texturing (TFEVT) method for micro-dimple pattern process. Int J Mach Tools Manuf 116:77–95
8. Kurniawan R, Ali S, Park KM, Jung ST, Ko TJ (2019) Experimental study of microgroove surface using three-dimensional elliptical vibration texturing. J Micro- Nano- Manuf 7(2):1–7
9. Nath C, Rahman M, Neo KS (2009) A study on ultrasonic elliptical vibration cutting of tungsten carbide. J Mater Process Technol 209:4459–4464
10. Silberschmidt VV, Mahdy SMA, Gouda MA, Naseer A, Maurotto A, Roy A (2014) Surface-roughness improvement in ultrasonically assisted turning. Procedia CIRP 13:49–54
11. Nath C, Rahman M, Andrew SSK (2007) A study on ultrasonic vibration cutting of low alloy steel. J Mater Process Technol 192-193(4):159–165
12. Chen Z, Yun S (2019) Design and kinematic analysis of a novel decoupled 3D ultrasonic elliptical vibration assisted cutting mechanism. Ultrasonics 95:79–94
13. Chen Z, Yun S (2019) A novel design method for 3D elliptical vibration-assisted cutting mechanism. Mech Mach Theory 134:308–322
14. Yang Y, Yayue P, Ping G (2017) Structural coloration of metallic surfaces with micro/nano-structures induced by elliptical vibration texturing. Appl Surf Sci 402:400–409
15. Zhichao Y, Lida Z, Guixiang Z, Chenbing N, Bin L (2020) Review of ultrasonic vibration assisted machining in advanced materials. Int J Mach Tools Manuf 156:103594
16. Xiaoming L, Binliang H, Zhijin Z (2014) Research on unidirectional ultrasonic vibrations turning7075-T6 aluminum alloy surface quality and morphology. J Hunan Univ Sci Technol (Nat Sci Ed) 29(2):28–30 (in Chinese)
17. Jinglin T, Junshuai Z, Peng C, Bo Z (2020) Effect of ultrasonic elliptical vibration turning on the microscopic morphology of aluminum alloy surface. Int J Adv Manuf Technol 106:1397–1407
18. Weihai H, Deping Y, Xinquan Z, Min Z, Dongsheng C (2018) Ductile-regime machining model for ultrasonic elliptical vibration cutting of brittle materials. J Manuf Process 36:68–76
19. Mingming L, Hao W, Liang G, Jieqiong L, Yan G, Bin C, Dongpo Z (2018) Modeling and analysis of surface topography of Ti6Al4V alloy machining by elliptical vibration cutting. Int J Adv Manuf Technol 98(9-12):2759–2768
20. Chen Z, Guilin S, Kornel FE (2017) Investigation of hybrid microtexture fabrication in elliptical vibration-assisted cutting. Int J Mach Tools Manuf 120:72–84
21. Chao K, Dazhong W (2018) Numerical investigation of the performance of elliptical vibration cutting in machining of AISI 1045 steel. Int J Adv Manuf Technol 98:715–727
22. Teng C, Dong L, Rong S, Guowen P, Yongbo W (2018) Simulation on surface micro texture of aluminium alloy based on ultrasonic elliptical vibration cutting. J Shaanxi Normal Univ (Nat Sci Ed) 46(4):50–57 (in Chinese)
23. Lusheng Y, Bo Z, Yi W, Chongyang Z (2019) Study on surface micro-texture characteristics of 7075 aluminum alloy by elliptical vibration assisted cutting. Chin Mech Eng. http://kns.cnki.net/kcms/detail/42.1294.th.20191113.1450.029.html (in Chinese)
24. Xinquan Z, Senthil Kumar A, Rahman M, Nath C, Kui L (2011) Experimental study on ultrasonic elliptical vibration cutting of hardened steel using PCD tools. J Mater Process Technol 211(11):1701–1709
25. Wule Z, Yu H, Kornel FE, Zhiwei Z, Bingfeng J (2017) Modeling of the effects of phase shift on cutting performance in elliptical vibration cutting. Int J Adv Manuf Technol 92:3103–3115
26. Yu'an J, Jun P, Guang Y, Tao J, Zhihuang S (2019) Influence of ultrasonic elliptical vibration cutting trajectory change on surface morphology. Acta Armamentarii 40(10):2170–2176
27. Cunying Z, Bo Z, Xiaobo W (2019) Modeling and experiment of surface microstructure by longitudinal-torsional compound ultrasonic end milling. Surf Technol 48(10):52–63 (in Chinese)

Publisher's note Springer Nature remains neutral with regard to jurisdictional claims in published maps and institutional affiliations.